Available online at www.sciencedirect.com
SCIENCE DIRECT®
Journal of Power Sources 139 (2005) 141–151
JOURNAL OF POWER SOURCES
www.elsevier.com/locate/jpowsour

Synthesis, characterization, and conductivity measurements of hybrid membranes containing a mono-lacunary heteropolyacid for PEM fuel cell applications

David R. Vernon[d], Fanqin Meng[a], Steven F. Dec[b], D.L. Williamson[c], John A. Turner[d], Andrew M. Herring[a,*]

[a] *Department of Chemical Engineering, Colorado School of Mines, Golden, CO 80401-1887, USA*
[b] *Department of Chemistry and Geochemistry, Colorado School of Mines, Golden, CO 80401-1887, USA*
[c] *Department of Physics, Colorado School of Mines, Golden, CO 80401-1887, USA*
[d] *Hydrogen and Electricity, Systems and Infrastructure Group, National Renewable Energy Laboratory, Golden, CO 80401-3393, USA*

Received 18 June 2004; accepted 15 July 2004
Available online 15 September 2004

Abstract

Hybrid inorganic/organic membranes using a lacunary heteropolyacid proton conductor, $H_8SiW_{11}O_{39}$, in stable polymer matrices based on polyethylene glycol were prepared by a sol–gel method. NMR and IR measurements indicate that this improved sol–gel membrane contains robust covalent bonds between the proton conductor and polymer backbone. However, the polymer in these model systems is not expected to be oxidatively stable. Diffusion coefficients measured for this material, $1.2 \times 10^{-6}\,cm^2\,s^{-1}$, are of the same order of magnitude as for to that of Nafion® whilst ion exchange capacities, 2–2.5 meq g^{-1}, are twice that of Nafion® 117. The temperature dependence of the conductivity increases exponentially with temperature. However, fuel cell performance of this material is poor when compared to a Nafion® 117 membrane electrode assembly (MEA). One possible explanation is that there is a lack of organization of the proton conducting elements in the hybrid material. In addition, ex situ membrane conductivity measurements compared to in situ MEA polarization measurements reveal large interfacial resistances in the hybrid membrane MEAs. Further, it appears that these membranes, as currently formulated, require quite stringent humidification requirements for maximum performance.

Keywords: Fuel cell; Heteropolyacid; Proton exchange membrane; Hybrid nano-composite; Membrane electrode assembly

1. Introduction

Proton exchange membrane (PEM) fuel cells represent a promising energy source for automobiles, stationary applications and portable devices [1]. However, the PEM fuel cells currently available perform optimally at 80 °C, as the perfluorosulfonated polymer membranes, on which they are based, must be fully hydrated for maximum proton conduction, a condition not achievable at ambient pressure above 100 °C [1]. For many applications, operation of PEM fuel cell above 80 °C is highly desirable. Elevated temperature operation will facilitate the use of hydrogen produced via reforming of hydrocarbons with higher CO content than can be currently utilized, leading to simplifications of the reformer [2]. For vehicular applications an operating temperature of 120 °C [3] will allow heat rejection via existing radiator technology and for stationary applications, operating temperatures up to 200 °C will allow the fuel cell to be more efficiently integrated into combined heat and power applications. It has been a grand challenge for the PEM fuel cell community to

* Corresponding author.
E-mail addresses: jturner@nrel.gov (J.A. Turner), aherring@mines.edu (A.M. Herring).

0378-7753/$ – see front matter © 2004 Elsevier B.V. All rights reserved.
doi:10.1016/j.jpowsour.2004.07.027

develop fuel cells capable of operation at temperatures above 100 °C. In addition, reducing or eliminating the need for external humidification would yield significant reductions in complexity, weight and cost of fuel cell systems [1].

With this in mind, the search for efficient proton conducting membrane materials has mainly focussed on the following systems: sulfonated polymers [4], phosphoric acid imbibed polybenzimidazoles (PBI) [5], and hybrid membranes containing inorganic super acids [6–8]. Of the inorganic super acids, the heteropolyacids (HPA) are a large and structurally diverse group of materials [9] that are known to have high proton conductivities at ambient temperatures [10] and have the potential for high-temperature PEM fuel cell operation [11]. Only the four commercially available HPA based on the Keggin structure [12]: 12-phosphotungstic, 12-phosphomolybdic, 12-sillicotungstic, and 12-sillicomolybdic acids have been studied to any great extent and the study of proton conduction in these materials has been limited [11,13,14]. There is, therefore, a need to correlate proton conductivities of the HPA with the vast number of structures and hydration states available as well as devise ways to incorporate the HPA into optimized material for fuel cell operation. Among others, mechanical robustness, chemical stability, and retention of HPA are the main challenges in preparing HPA-containing membrane materials. Many brute force solutions to the heteropolyacid retention problem result in isolation of the HPA and do not allow proton communication through the membrane. The HPAs must be retained in such a way that they will not be coated with an inactive material and will be in close enough proximity to each other to easily exchange protons all the way through the membrane. Optimization of HPA loading, polymer matrix characteristics and robust film formation are continuing development tasks. Various approaches to incorporate HPA into fuel cell ready membranes have been attempted including fabricating unsupported HPA pellets [15], doping Nafion® [16–18] or other sulfonated polymers [19,20], doping PBI [21,22], and sol–gel methods [7,23–27].

In the search for desirable proton exchange membrane materials, we became interested in the work of Honma et al. on silica based sol–gel HPA-hybrid membranes, wherein the organic/inorganic hybrid materials were synthesized via a convenient sol–gel route by doping heteropolyacid (12-phosphotungstic acid) into a cross-linked silicate-polyether matrix [7,8,23–25,27–29]. In this work a variety of sol–gel HPA-containing membranes have been prepared in which proton conductivities up to 0.01 S cm^{-1} have been measured by AC impedance spectroscopy at temperatures up to 165 °C, and 100% RH but little further characterization of the mechanism of proton conduction has been carried out and there have been few attempts to study these membranes in membrane electrode assemblies (MEAs). The HPA was used as an acid catalyst in the synthesis and as a proton carrier in the resultant membrane. In such a material, positively charged aggregates presumably form within the cross-linked silica network, to which heteropolyanions can bind via electrostatic interactions. However, to obtain higher chemical stability of the hybrid material, covalent bonding between the heteropolyanion and the organic skeleton is more desirable. We, therefore, modified the method of Honma et al., to fabricate covalent bonds between the HPA and the organic matrix.

For the most readily available and frequently investigated HPA, such as 12-phosphotungstic acid (12-PWA) and 12-sillicotungstic acid (12-SiWA), the spherical-shaped anion contains 12 tungsten atoms, each of which are bonded to six oxygen atoms in a pseudo-octahedral geometry, leaving no coordination site for other ions or atoms. In comparison, the lacunary Keggin anions $[XW_{12-m}O_{39}]^{n-}$ (m = 1, 2 or 3) have one or more vacant positions available for bonding with their unshared oxygens. Generation of such vacant sites makes the anions possible penta- or tetra-dentate ligands towards other transition metal cations—a large number of transition metal complexes of this type are known. In addition, complexation with organic molecules through Si–O covalent bonds at the lacunary site has also been reported [30–34]. By using $H_8SiW_{11}O_{39}$, $HSiW_{11}$ (Fig. 1), a mono-lacunary Keggin type HPA, we hoped to covalently bond the HPA to the hybrid silica polymer rather than simply entrap it in the silica domains of the material as was achieved earlier [7,23–25,35].

Using $HSiW_{11}$, our hybrid HPA membrane development has reached the stage where these materials can be fabricated into membrane samples suitable for fabrication into MEAs, and tested under fuel cell conditions. Although these hybrid membranes are still not mechanically robust enough for long-term fuel cell use and are probably not oxidatively stable, as they contain C–H bonds, the membranes were further investigated as important models for HPA proton conducting systems, which are a potential alternative to the perfluorosulfonated polymer membranes such as Nafion®.

MEA fabrication is a separate development task, and fabrication techniques need to be optimized for the new membrane materials. In this study we undertake the comparison of a standard Nafion® 117 MEA to two hybrid HPA membrane-based MEAs. Standard techniques were used to fabricate the MEAs using the same electrode materials and the same fabrication conditions. We compare measurements of ex situ membrane conductivity and in situ MEA polarization in order to evaluate the bulk membrane resistance and the electrode/membrane interfacial resistance. This comparison tells us whether standard MEA fabrication techniques are suitable for these very different types of membranes and gives us clues for the further optimization of both the MEA fabrication techniques and the membrane synthesis.

2. Experimental

2.1. Membrane synthesis

Precursor materials polyethylene glycol (M_n = 400), PEG400, $Na_2SiO_3{\cdot}9H_2O$, monophenyltriethoxysilane (MPhTEOS) (98%), and Amberlite IR-120 were purchased

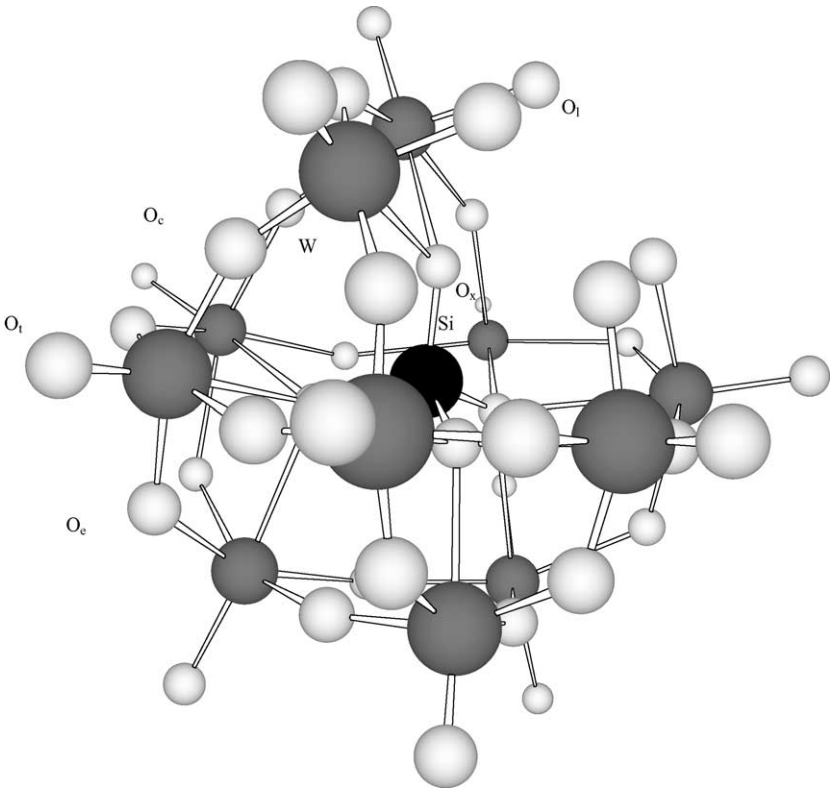

Fig. 1. Ball and stick representation of $H_8SiW_{11}O_{39}$ with the different oxygens labeled: x, Si-O; t, terminal W=O; e, edge shared; c, corner shared; l, lacunary.

from Aldrich. Na_2WO_4 was purchased from Fisher Scientific. 3-Isocyanatopropyltriethoxysilane (ICPTEOS) (95%), was purchased from Gelest. All materials were used as supplied.

The synthesis of $H_8SiW_{11}O_{39}$, 11-SiWA, started from the potassium salt of the lacunary anion, $K_8[\alpha\text{-}SiW_{11}O_{39}]$ [36]. Then, the lacunary salt was reacted with Cu^{2+} ion to yield the copper complex [37], which was then passed through an Amberlite IR-120 column in the proton form to obtain the free acid. Powder X-ray diffraction pattern indicated the compound adopts the cubic Keggin structure and ICP-AA analysis gave a W:Si ratio of 10.9(4):1.

The following sol–gel and membrane synthesis was based on Honma's reported method [27]. PEG400/SiO_2 sol–gel precursor was prepared by reacting PEG400 with a stoichiometric amount of 3-isocyanatopropyltriethoxysilane at 60–70 °C for 5 days under N_2 atmosphere. The molecularly hybridized precursor thus-obtained was then hydrolyzed and condensed with the addition of $H_8SiW_{11}O_{39}$, which served as a catalyst as well as a proton dopant. MPhTEOS was added to the above mixture immediately under rapid stirring. Relative to the weight of the PEG400 precursor, 30% of $H_8SiW_{11}O_{39}$ and 60% of MPhTEOS were added. The transparent and slightly brownish free-standing membranes were obtained and stored in air before further tests. The two membrane samples tested in this work were made with the same composition; the only difference being that for membrane 1 (M-1), MPhTEOS was added without simultaneous stirring, while membrane 2 (M-2) was made by adding Mph under rapid stirring. M-1 is slightly thinner with coarser texture on the surface than M-2. The membrane characterization reported below is for M-1. As a control, membranes were also prepared by replacing HPA with HCl.

MPhTEOS was used to improve the chemical stability and hydrophobicity of the membrane [27]. MPhTEOS and PEG400 precursor share the same functional groups ($-Si(OEt)_3$), which can undergo hydrolysis and condensation with an acid catalyst. Because of the bulky phenyl group at the end of the molecule, MPhTEOS is believed to end cap the silane groups of the PEG400 precursor, terminating the silica condensation and making the resultant membrane more hydrophobic.

2.2. Membrane characterization

The membrane sample and the control were characterized by attenuated total reflection (ATR), infrared spectroscopy using a Thermo Nicolet Nexus 670 FT-IR spectrometer with a 2 cm^{-1} resolution equipped with a Specac GS1100 ATR attachment with a KRS-5 multiple bounce crystal. Data were collected and worked up using the Thermo-Nicolet Omnic® 6.0 software package and were not corrected.

MAS ^{29}Si NMR spectra were recorded on a two-channel Chemagnetics CMX Infinity 400 NMR spectrometer operating at 79.4 MHz, using a Chemagnetics 7 mm double-

resonance MAS probe equipped with a Pencil spinning module, sample spinning at 5 kHz.

Proton diffusion measurements were obtained on a Chemagnetics Infinity 400 NMR spectrometer operating at 400 MHz for ^{1}H using a 5 mm Doty Scientific, Inc., #20–40 z-gradient pulsed-field gradient NMR probe. The stimulated-echo pulse sequence was used [38]. Spectra were recorded as a function of gradient pulse current using a 90° radio frequency excitation pulse of 6.5 μs, a gradient pulse width of 1.0 ms and a gradient pulse spacing of 3.2 ms. In order to minimize eddy currents generated by switching the gradient pulses on and off, a trapezoidal gradient pulse shape with a ramping time of 0.5 ms was used [39]. The gradient coil was calibrated using water at 25 °C and was found to have a strength of 19 Gauss cm^{-1} A^{-1}. Spectra were recorded for 40 equally spaced values of gradient coil currents between 0.3 mA and 15 A in a random array by signal averaging 16 transients. The resulting NMR spectra were integrated and fit into a two-Gaussian decay using Spinsight® software available from Varian, Inc. The temperature of the sample was calibrated using a type-T thermocouple inserted into a sample of alumina in the NMR probe. To maintain a steady hydration state of the membrane, samples were sealed with a torch under vacuum in a NMR tube with a drop of water at the bottom of the tube; a gap of 27 mm between the bottom of the NMR tube and the lower end of the membrane sample permitted the sample to be placed in the NMR and gradient coils while minimizing the signal from the liquid water.

Small angle X-ray scattering (SAXS) experiment was performed with a Kratky system [40] attached to a Rigaku rotating Cu anode X-ray generator. The Cu-Kα X-rays (λ = 0.15418 nm) were obtained using a graphite monochromator. X-ray scattering data were collected in a step-scanning mode over a range in 2θ from 0.13° to 8.8°, corresponding to momentum transfer range (q) from 0.09 to 6 nm^{-1}. Data reduction was performed by literature procedures [41]. A background profile was taken with no membrane in the X-ray beam and was subtracted from the sample.

Cross-section transmission electron microscope (TEM) images were obtained using a Philips Tecnai G2 instrument, with beam strength of 80 kV. A small slice of membrane sample was first swollen in water for one day (Milipore water was used in all the following steps of the TEM experiment), followed by soaking in saturated lead acetate for another day. Then, the sample was briefly washed with water, put between two glass slides and dried under vacuum for one day. The dried sample was imbedded in epoxy, cured at 60 °C for one day, and then cut down to <100 nm in thickness using a microtome. Finally the above-treated sample was placed on a 400-mesh copper grid and TEM images of the cross-section were taken.

Apparent ion exchange capacity (IEC) of the membrane was measured using a simple acid–base titration method. Approximately 200 mg of membrane sample was first washed with water, blotted with Kimwipes and then dried at ~50 °C for about 30 min before weighing on an analytical balance. Then, the weighted sample was soaked in 15.00 mL of standardized NaOH solution (~0.1N), 5.00 mL of which was taken after 24 h for titration with standardized HCl (~0.1N). Nafion® 117 was used as a control to validate the measurement. Apparent IEC was calculated as follows:

$$\mathrm{IEC(meq)} = \frac{3((5.00 \times N_{\mathrm{NaOH}}) - (V_{\mathrm{HCl}}(\mathrm{mL}) \times N_{\mathrm{HCl}}))}{\text{sample weight(g)}}.$$

2.3. Ex situ membrane conductivity measurements

The ex situ membrane conductivity measurements were made using a Bekktech four-point conductivity cell. A VoltaLab potentiostat/galvanostat, model number PGZ 301, was used to apply a linearly stepped current between the two platinum mesh outermost electrodes and the voltage drop was measured between the innermost electrodes which are a known distance apart (Fig. 2). Membrane samples approximately 2 cm in width were held in the four-point probe apparatus in humidity- and temperature-controlled hydrogen gas. The resistance of the sample was calculated from the current and voltage drop based upon the distance between the two innermost electrodes. Sample thickness measurements and width measurements were made using a Mitutoyo digital micrometer and caliper, respectively. The resistivity and conductivity of the membrane materials were calculated using the voltage, current, sample thickness and width measurements. The humidification levels were kept at 100% humidity up to a cell temperature of 80 °C for all conductivity tests. The membrane samples were allowed to equilibrate with the humid gases in the test cell for a minimum of 1 h before measurements were taken.

2.4. MEA fabrication

Catalyzed E-TEK ELAT® electrodes with 0.35 mg Pt cm^{-2} loading of 20 wt % Pt on Vulcan XC-72 carbon on carbon cloth gas diffusion backings with an active area of 5 cm^2 were used for MEA fabrication. MEAs were fabricated by a standard hot press method [42]. The electrodes were pretreated by brushing with one coating of 5% Nafion® solution in mixed alcohols, supplied by Electrochem Inc., and allowed to dry for 45 min under ambient conditions. The 5 cm^2 electrodes were then hot pressed onto the membranes at 130 °C with a force of 360 psi for 90 s. The MEAs were removed

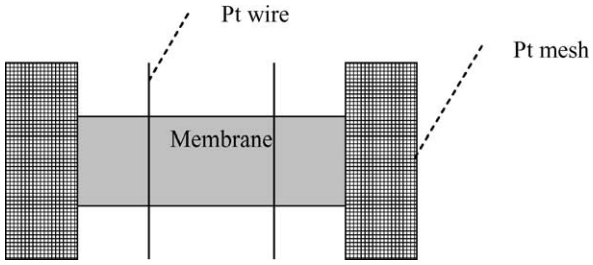

Fig. 2. Bekktech conductivity cell schematic.

from the hot press and allowed to cool for 15 min under a 5 lb weight. Good mechanical electrode adhesion was achieved with both the Nafion® membrane and the experimental membranes.

2.5. Polarization curves

The MEAs were then tested with humidified hydrogen and oxygen to obtain polarization curves. The MEAs were tested using a GlobeTech test station controlled using Scribner and Associates FuelCell software, version 3.2D. For greater accuracy at low currents generated by the hybrid membrane samples, an EG&G VersaStat II potentiostat was used, controlled with Powersuite software. The Nafion® MEA polarization curves were collected in a voltage-controlled mode with discrete steps of 100 mV and a settling period of 60 s before taking each data point. The hybrid membrane MEA polarization curves were recorded continuously at a scan rate of 2 mV s^{-1}. The single cell test hardware was of standard design using single channel serpentine flow field. The cell hardware was compressed using eight quarter-twenty threaded bolts with a torque of 40 in-lb. All polarization curves were recorded with the humidifier bottles maintained at the same temperature as the cell, supplying 100% humidity. At low current densities, below 200 mA cm^{-2}, the flow rates of 100 sccm for hydrogen and 100 sccm for oxygen were maintained using the mass flow meters incorporated into the fuel cell test station. Both the anode and cathode flow fields were maintained at 30 psig pressure for the polarization curves, except the curve for experimental membrane number one which was only run at ambient pressure due to leak problems. All polarization curves were recorded in both the upward and downward direction.

3. Results and discussion

3.1. Membrane characterization

Hybrid membranes formed from silica end capped PEG400 and 11-SiWA are transparent and can be cast into transparent sheets of at least 8 cm × 8 cm squares. The membranes fabricated from the lacunary 11-SiWA when hydrated, appear mechanically more robust the membranes fabricated from 12-SiWA and are more easily fabricated into MEAs. From their air equilibrated state, the membrane materials absorbed 13–17 wt.% of water after 1 h of submersion at room temperature to give a membrane of 268 μm and the materials appeared to swell slower than Nafion® when in contact with a droplet of DI water. The materials both absorb methanol faster than water and tear/fracture easily after this treatment. After soaking in DI water for 1 h the materials also tear/fracture more easily. After drying overnight, 18 h, from the air equilibrated state the membranes lost 7.6–8.5% of their original weight indicating that they hold on to at least half their water strongly.

The ATR IR spectrum of a PEG400/SiO_2 hybrid membrane synthesized with HCl as the catalyst is shown in Fig. 3a. Bands assigned to υ(OH) and δ(OH) are observed at 3322 and 1695 cm^{-1}, respectively. The organic polymer is assigned to υ(CH) bands at ca. 2870 cm^{-1} and a complex series of bands below 1600 cm^{-1}. The silica in this material has υ(SiO) bands at 1090 and 1043 cm^{-1}.

The ATR of a dry membrane prepared using 11-SiWA is shown in Fig. 3b. The bands of the υ(WO) are now seen as distinct bands below 1100 cm^{-1} [43]. The $\upsilon(SiO_x)$ band is seen as a sharp band at 1028 cm^{-1}, superimposed on the υ(SiO) band at 1043 cm^{-1}. Three bands are observed for the $\upsilon(WO_t)$ 969, 918, and 882. The $\upsilon(WO_c)$ is assigned to a band at 799 cm^{-1} with a shoulder and the $\upsilon(WO_c)$ to a pair of bands at 742 and 730 cm^{-1}, The $\upsilon(WO_l)$ is observed at 699 cm^{-1} much lower than commonly observed for other skeletal υ(WO) of Keggin anions [44]. New sharp bands are observed at 1594 and 1429 cm^{-1} assigned to $\upsilon(SiO_lW)$. Interestingly the υ(CH) band as compared to the control (Fig. 3a) is distinctly split into two bands, 2936 and 2867 cm^{-1}, indicating a different configuration of the polymer backbone. As the membrane is hydrated (Fig. 3c and d), a broad υ(OH) grows in at 3369 cm^{-1} together with a δ(OH) at 1644 cm^{-1} consistent with the presence of H_3O^+ in the hydrated material [44]. The material did not leach HPA on treatment in water at 80 °C as observed by ATR IR (not shown).

MAS ^{29}Si NMR experiment of the membrane showed four peaks, at −57.6, −65.3, −78.2, and −84.9 ppm, respectively. According to the literature [32,36,45], the peaks at −57.6 and −65.3 ppm are due to the RSi− group that is bonded to the lacunary Keggin anion through Si–O–W bridges, and the resonance at approximately −85 ppm has been consistently seen for SiO_4 in the center of 12-SiWA as well as the lacunary (9-, 10-, and 11-SiWA) Keggin anions. The peak at −78.2 ppm is assigned to hydrolyzed phenylated silica.

TEM images were taken of the membrane, which showed a uniform surface with a uniform distribution of tungsten as measured by EDX. This result from powder X-ray diffraction measurement of the membrane, shows very little crystallographic ordering of the membrane. When the membrane was stained with lead acetate in aqueous solution as shown in Fig. 4, isolated regions of high contrast, 5–6 nm in diameter, are randomly dispersed in the organic matrix. This observation leads us to conclude that the swollen membrane has isolated regions of hydration, no obvious channels are observed in the material. In addition, larger lead stained features <50 nm where observed suggesting that the membranes may have performance-degrading cracks on the microscopic scale.

Fig. 5 shows SAXS data from the 11-SiWA-doped sample (upper curves) and the control membrane (lower plot) where HCl, instead of 11-SiWA, was used in the membrane synthesis. Interestingly, in addition to the typical SAXS curve at the low angle region, the HPA-containing sample showed a pseudo-Bragg-type peak in the higher q range, which is suggestive of a certain degree of ordering of the particles or some

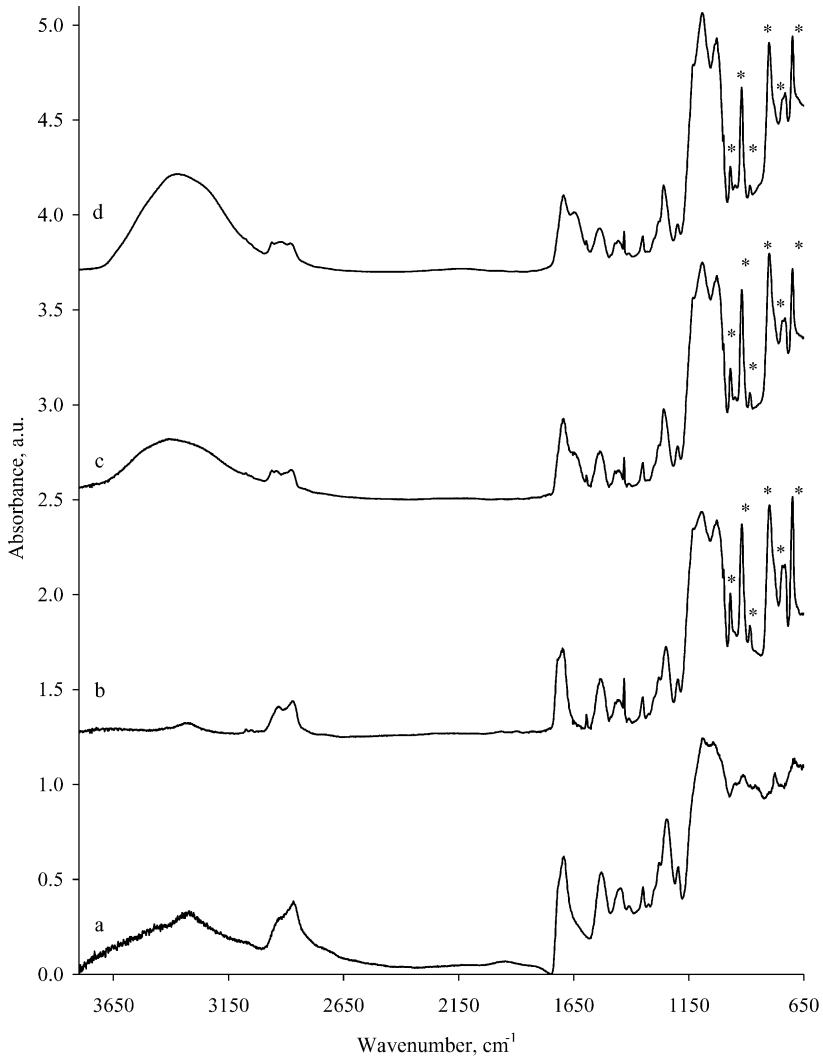

Fig. 3. ATR spectra of PEG400/SiO_2 hybrid membranes, (a) membrane made with HCl as a control, membrane synthesized using $HSiW_{11}$ as catalyst and constituent, (b) dry sample, (2) sample soaked in water for 30 min, (c) sample soaked in water for 3 h, (d) (*) HPA peaks.

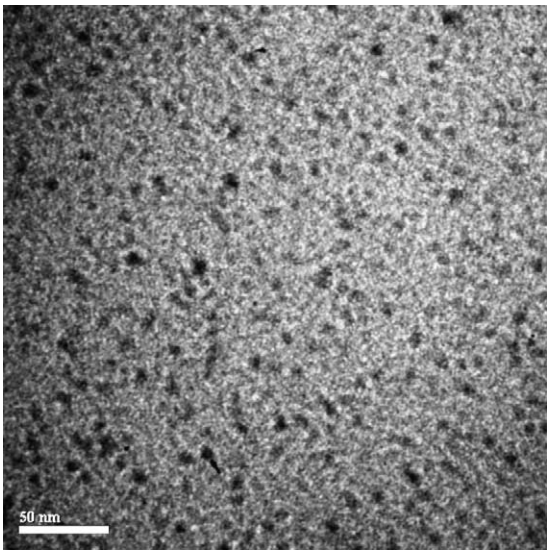

Fig. 4. TEM image of sol–gel membrane, scale bar 50 nm.

crystallinity. As shown by the solid line, a fit of a narrow distribution of spheres with an average diameter of 2.0 nm yields a good fit to the lower-q portion of the curve. The slight discrepancy between the experimental data and the fitting at the lowest q is due to interparticle interference. Based on the position of the Bragg-like peak (q_p = 4.32 nm^{-1}), an interplanar spacing, d = 1.51 nm, is calculated from the Bragg law ($d = 2\pi/q_p$). The control membrane also yielded a peak at a slightly higher position, corresponding to d = 1.23 nm.

Considering the composition of the control membrane, condensed organic silica particles are the only species that can scatter X-rays strongly enough to give rise to the Bragg-like peak: particles comprised of other elements including carbon, oxygen and hydrogen could not be seen by X-ray so clearly. According to well-known crystal data of the Keggin anion, the monovacant lacunary anion used in this study, 11-SiWA, has a diameter of approximately 1.0 nm. Therefore, the objects responsible for the SAXS curve are very likely 11-SiWA wrapped by organic silica network. This in-

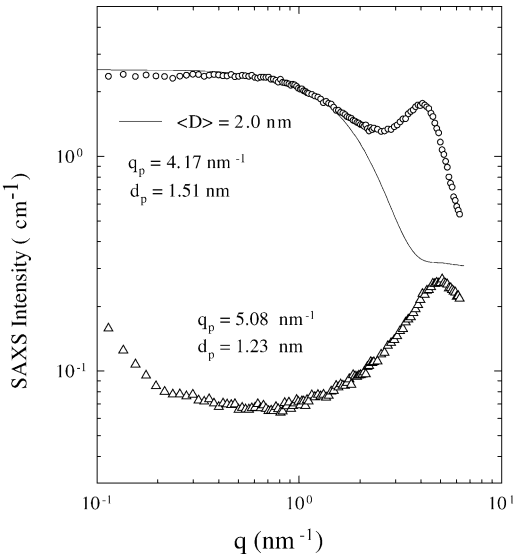

Fig. 5. SAXS data from 11-SIWA-doped membrane (upper) and HCl-catalyzed control (lower). Broken curves are experimental data, and solid line is the Guinier approximation fitting.

terpretation is reasonable, judged by the comparable intensity of the two peaks: if the SAXS curve is caused by pure 11-SiWA particles, which have much higher electron density than organic silica, one would expect it to be much stronger than the pseudo-Bragg peak from the silica particles. The SAXS studies reveal a picture of the structure of our membrane material: silica-11-SiWA particles are randomly dispersed in the organic matrix, and the organic silica particles are packed in semi-crystalline arrays with sizable interplanar spacing.

3.2. Ex situ membrane conductivity results

Proton diffusion as measured by PFGSE experiments indicated the importance of hydration—membrane samples sealed in a dry tube did not give rise to measurable diffusion signals. Samples sealed with a drop of water in the NMR tube also gave no measurable proton diffusion immediately after sealing. However, this 'wet' sample gave increasingly faster diffusion coefficients after aging (Table 1). As the membrane slowly swelled with water, a diffusion coefficient of 2.0×10^{-7} cm^2 s^{-1}, corresponding to the silica/HPA protons, 83% of the sample, was measured after 1 week, the remaining 17% of the membrane having a diffusion coefficient ca. 3×10^{-5} cm^2 s^{-1}, as expected for water in the membrane. After 3 weeks and further swelling of the membrane, the more hydrated silica/HPA protons in the membrane diffusion coefficient had increased to 1.2×10^{-6} cm^2 s^{-1}, corresponding to 50% of the sample. Fifty percent of the protons in the sample now had a diffusion coefficients ca. 3×10^{-5} cm^2 s^{-1}, as expected for the increased amount of water in the membrane. By comparison we have measured the diffusion coefficient of protons in Nafion® 117 as 6.8×10^{-6}, demonstrating that diffusion coefficients in these hybrid materials can be on the same order of magnitude as commercial ion exchange membranes.

Table 1
Diffusion coefficients of the hybrid PEG400/SiO_2/11-SiWA membrane measured by PFGSE NMR (cm^2 s^{-1}) at room temperature

Time	<1 day	1 week	3 weeks
Protons in membrane	0	2.0×10^{-7} (83%)	1.2×10^{-6} (50%)
Water in membrane	na	2.6×10^{-5} (17%)	3.2×10^{-5} (50%)

Apparent ion exchange capacities of the membrane materials were determined to be in the range of 2.0–2.5, twice that of Nafion® 117. Such high IEC coupled with fast proton diffusion should be very promising for high proton conducting properties.

The dc ex situ membrane conductivity measurements showed that the conductivity of Nafion® 117 at 80 °C was approximately an order of magnitude higher than the conductivity of our sol–gel hybrid membranes, as shown in Fig. 6, in which data for two different preparations of the hybrid membrane are compared to Nafion® 117. The Nafion® 117 samples showed very slightly increasing conductivity with increasing temperature up to 80 °C, increasing approximately 1.7 times from room temperature 20 to 80 °C with the change from 30 to 80 °C being 1.6 times. The hybrid membrane sample showed much larger increase in conductivity with increasing temperature, the increase from 22 to 80 °C being 225 times and the increase between 30 and 80 °C being 13.86 times. The maximum value for the proton conductivity achieved by us, 0.01 S cm^{-1} by dc conductivity is comparable to those obtained for similar systems, by ac impedance spectroscopy [7]. In fact the best fit to the data for the hybrid samples was an exponential fit (Fig. 6), although the scatter in the data was large; this may have been because the hybrid membranes took an unexpectedly large time to reach equilibrium in the presence of water. The hybrid membranes show a large increase in conductivity with longer equilibration times as observed for the PFGSE NMR measurements. Unfortunately measurements above 80 °C were not possible for the two hybrid membranes due to the membrane tension required by the conductivity cell and mechanical instability issues in these membranes at high temperatures under high humidity conditions.

3.3. In situ polarization results

The polarization performance of the hybrid membranes was very low as is expected for initial trials of MEA fabrication with new membrane materials (Fig. 7). Mechanical degradation and electrode delamination amongst a number of possible degradation mechanisms limited testing time and the range of testing conditions that could be studied. The polarization performance of the experimental membrane MEAs were dominated by resistance effects and did not show characteristic kinetic- or mass transport- dominated regions. The polarization curves for a Nafion®117 benchmark were expected with the three polarization loss regions ascribed to

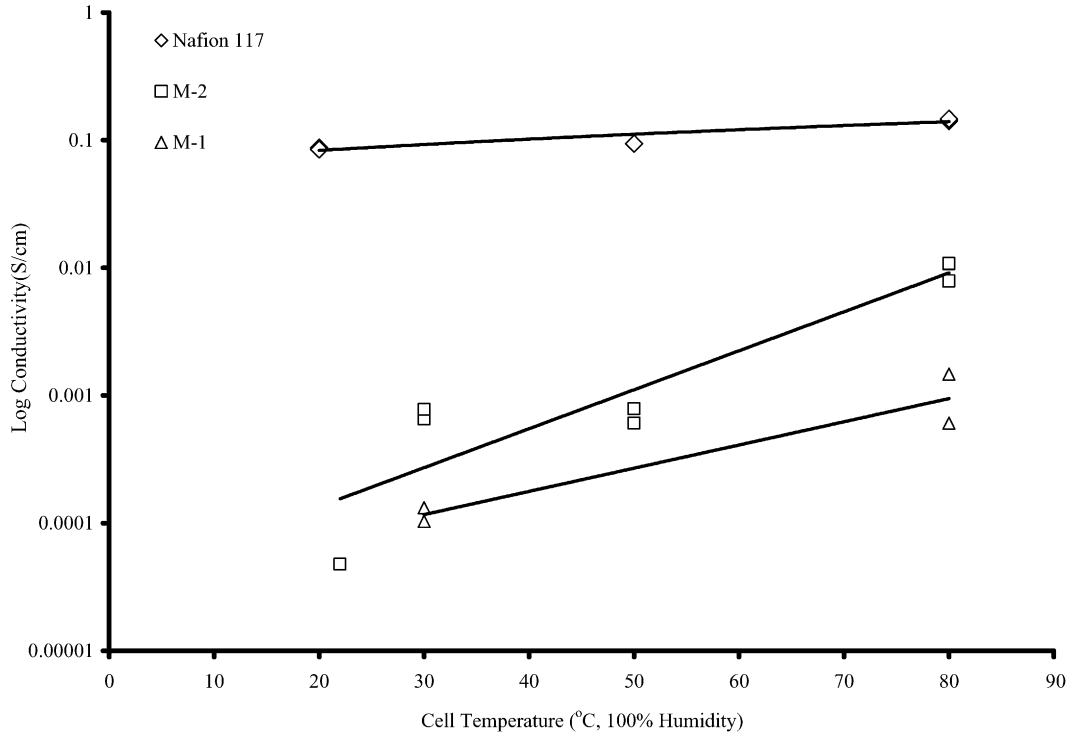

Fig. 6. DC conductivity of membrane samples vs. temperature all at 100% humidity. Trendline for Nafion® 117, for the hybrid membranes, M-1 and M-2, exponential.

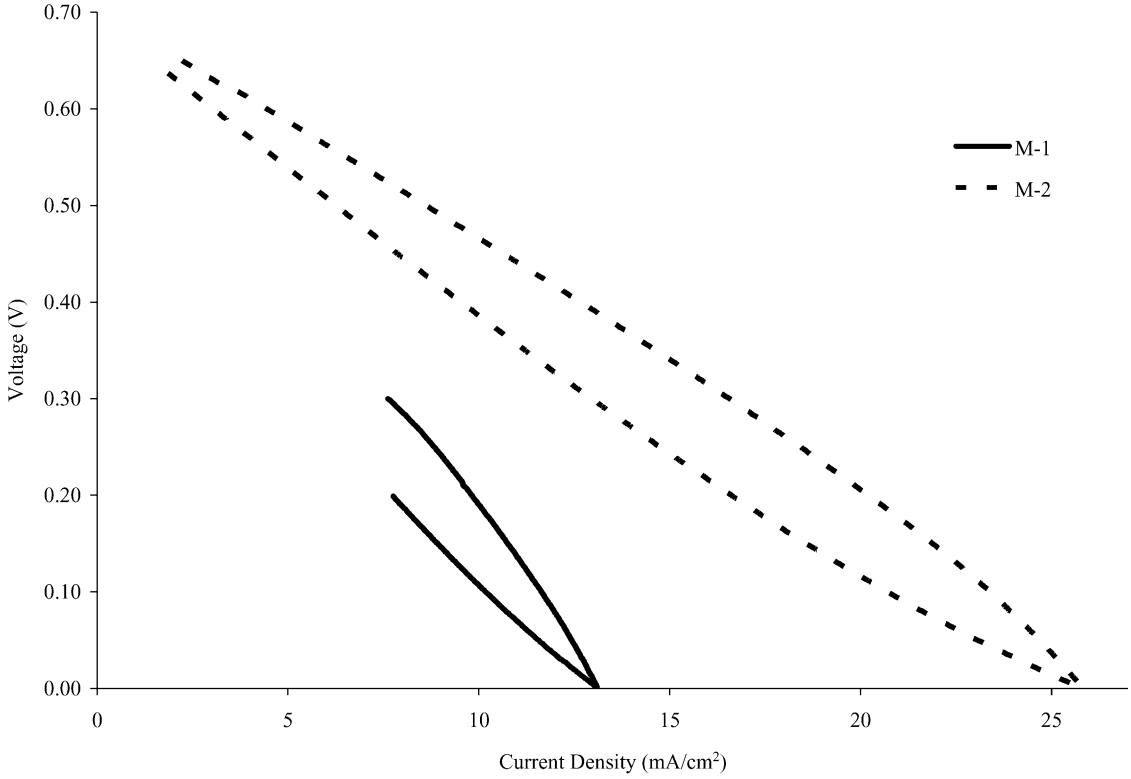

Fig. 7. Polarization curves for the two experimental hybrid membranes as MEAs at 80 °C, humidifiers at 80 °C.

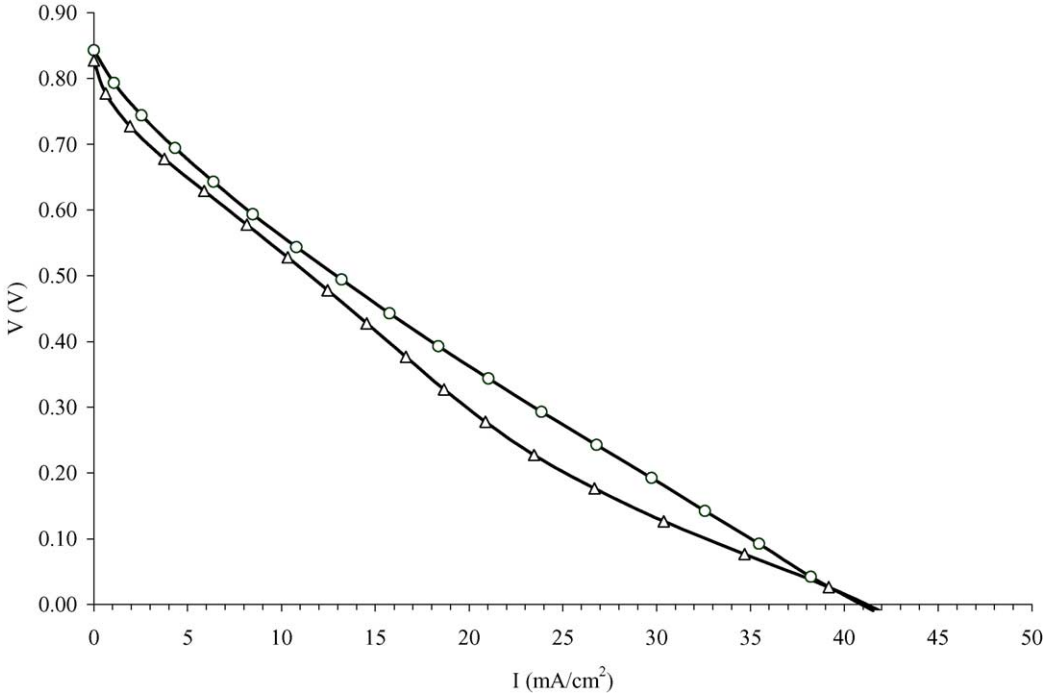

Fig. 8. Polarization curves for a membrane with a ratio of PEG400 precursor: $H_8SiW_{11}O_{39}$:MPhTEOS, of 100:40:100. △, plain E-tek electrodes; ◯, E-tek electrodes painted with Nafion® solution. Fuel cell at 47 °C, humidifier bottles at 80 °C.

kinetic, ohmic and transport clearly delimited with an OCV of 1.0 V and a current of 1.4 A cm^{-2} at 0.2 V.

The experimental membrane MEAs was tested across a range of conditions in order to find the optimum operating conditions. Fast degradation of the material in the fuel cell test hardware limited the number of tests, which could be performed at peak performance. A maximum open circuit voltage of 0.86 V was observed. The low open circuit values suggest issues with cross-over or electrical conductivity in the experimental MEA. The highest current produced in the experimental samples of membrane was obtained early in the testing process when higher temperatures of 80 °C were first reached. The lowest recorded polarization results for the membrane are shown below. The polarization runs with the lowest slope values generated the largest currents of all of the runs at any given voltage. This further supports the idea that the polarization performance is controlled by resistive effects in the hybrid MEA.

To try and improve the performance of the material, we synthesized a membrane with a higher loading of HPA, specifically PEG400 precursor:$H_8SiW_{11}O_{39}$:MPhTEOS, ratio of 100:40:100, M-3. This membrane, M-3, in which the HPA content is only 10% increased, showed almost twice the performance of the M-2 membrane at 80 °C, at 47 °C with saturated gases, its temperature of maximum performance (Fig. 8). However, the M-3 membrane gave no appreciable current at 80 °C.

3.4. Comparison of in situ and ex situ conductivity results

Ex situ membrane conductivity measurements are compared to in situ MEA polarizations across a range of currents (Fig. 9, Table 2). The polarization of the Nafion® 117 benchmark MEA was corrected for the membrane IR losses using the conductivity values measured in the ex situ conductivity cell. The difference between the membrane IR-corrected cell voltage and the open circuit voltage at the beginning of the scan was calculated to find the membrane IR-corrected polarization for the Nafion® 117 benchmark MEA. The same procedure was used to find the membrane IR-corrected polarizations for the MEA based on experimental membrane.

Table 2
Membrane IR-corrected polarizations for the two experimental membrane and Nafion® 117 MEAs across a range of different current densities

Membrane	Average IR-corrected polarization (mV) at current density (mA cm^{-2})				Nafion® normalized average IR-corrected polarization (mV) at current density (mA cm^{-2})			
	5	8	13.1	25.8	5	8	13.1	25.8
Nafion® 117	54	63	86	114				
M-1	na	194	338	na	na	3.1	3.9	na
M-2	121	125	151	379	2.2	2.0	1.8	3.3

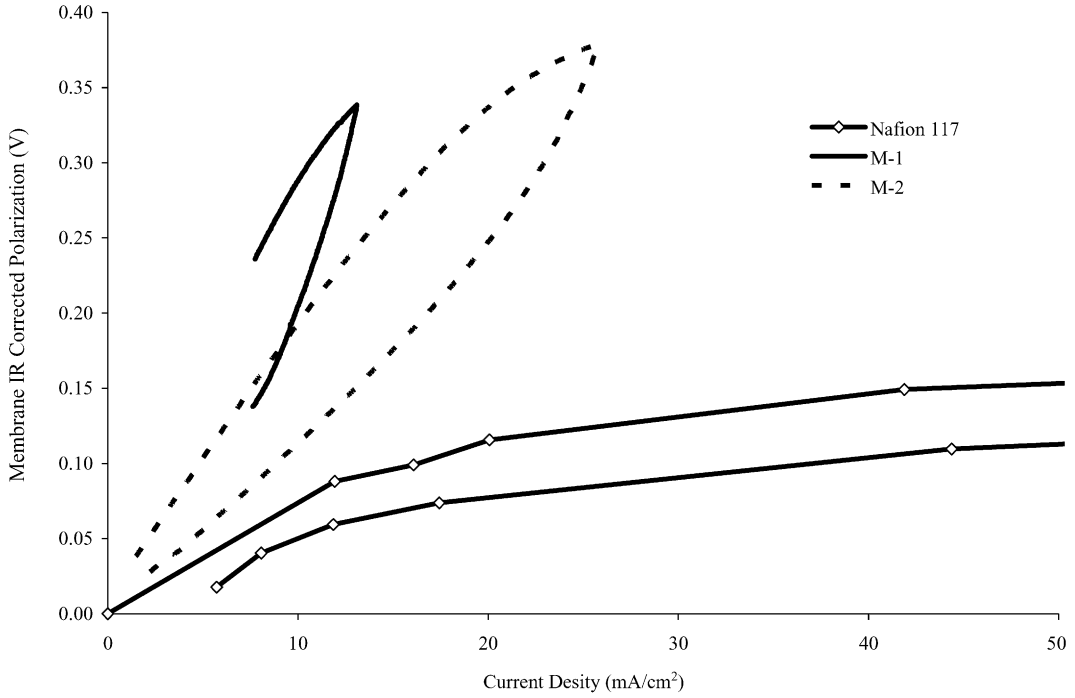

Fig. 9. Membrane IR-corrected polarizations for the two experimental membranes M-1 and M-2 and Nafion® 117 MEAs across a range of different current densities.

The experimental hybrid membranes had significantly higher IR-corrected polarizations even though the electrode materials, MEA fabrication procedure, humidification and the gas flow rates were the same. This suggests that the difference in performance between the experimental membrane and Nafion® is not solely the differences in bulk conductivity but is related to interfacial resistance between the Nafion® ionomer in the electrodes and the membrane materials. With this in mind optimization of MEA fabrication processes as well as the development of more compatible ionomer materials in the electrodes may produce very significant improvements in performance for the hybrid membrane MEA.

4. Conclusions

$H_8SiW_{11}O_{39}$, 11-SiWA, is incorporated into an inorganic–organic hybrid membrane and retained after soaking. This represents the first example of a heteropolyacid attached covalently to a polymer backbone in a proton exchange membrane. Large-area mechanically stable membranes can be made with this method. NMR and IR results from the mono-lacunary Keggin type HPA, $H_8SiW_{11}O_{39,}$ in the hybrid material are consistent with the proposed covalent bond formation. Diffusion measurements under dry and hydrating conditions suggested that humidification is necessary to achieve higher proton mobility, but when fully hydrated, the material can achieve proton diffusion coefficients as high as the commercial Nafion® 117 membrane (as measured by PFGSE). In addition, ion exchange capacities in the range of 2–2.5 meq g^{-1} were observed, suggesting that these hybrid materials are capable of very high proton conduction. However, TEM and SAXS experiments indicated the HPA particles are randomly dispersed in the polymer matrix and cannot communicate with each other effectively, possibly resulting in low fuel cell performance. Further work will be necessary in order to achieve appropriate organization of the proton conducting moieties in these materials.

Membrane electrode assemblies can be fabricated using hot press techniques to achieve good mechanical bonding of the electrodes to the experimental polymers. Drastically greater membrane IR-corrected polarizations for the experimental membrane MEAs as compared to the Nafion® benchmark MEA suggest very high interfacial resistance with the Nafion® ionomer in the electrode. Interfacial resistance with the electrode ionomer is one of the limiting factors of the performance of the experimental membranes.

In the future, development of a compatible ionomer will be necessary for optimum MEA fabrication. Continued testing may focus on the use of simple catalyst electrodes with no ionomer in order to more fairly compare the membranes to Nafion® membranes. These steps may significantly increase the performance of future experimental membrane MEAs.

The ex situ conductivity of the hybrid membranes increases more rapidly with increase in temperature compared to Nafion® 117 membranes. The increasing trend in conductivity of the hybrid membranes suggests that they may be developed for higher operating temperature applications. Humidification is required in these hybrid membrane systems; developing an understanding of the factors involved

in the need for humidification will play an important role in evaluating this future possibility.

Obviously this is a model system and the polymers used are not oxidatively stable in a fuel cell environment, which may explain the difficulty in obtaining reproducible polarization curves. Future work will focus on using more oxidatively stable polymer backbones in these systems.

Acknowledgements

This work was funded by a US DOE science initiative grant, DE-FC02-0CH11088. David Vernon thanks the National Renewable Energy Laboratory for support. We would like to thank the following individuals for useful discussions, Mr. Timothy Bekkedahl, Dr. H. Joachim Kleebe, Dr. Bradford Limoges, Ms. Jennifer Mahlers, Dr. Robert Moore, Dr. John Pern, and Ms. Mary Ann Sweikart. The lead acetate doped TEM images were obtained at Simon Fraser University, Burnaby, Canada, by Dr. Steven Holdcroft and Ms. Ana Siu who we would also like to thank for useful discussions.

References

[1] W. Vielstich, A. Lamm, H. Gasteiger (Eds.), Handbook of Fuel Cells—Fundamentals, Technology, Applications, Wiley, 2003.
[2] Q. Li, R. He, J.-A. Gao, J.O. Jensen, N.J. Bjerrum, J. Electrochem. Soc. 150 (2003) A1599.
[3] R.K. Ahluwalia, E.D. Doss, R. Kumar, J. Power Sources 117 (2003) 45.
[4] S.M. Haile, Acta Materialia 51 (2003) 5981.
[5] Y.-L. Ma, J.S. Wainright, M.H. Litt, R.F. Savinell, J. Electrochem. Soc. 151 (2004) A8.
[6] D.A. Boysen, T. Uda, C.R.I. Chisholm, S.M. Haile, Science 303 (2004) 68.
[7] I. Honma, H. Nakajima, O. Nishikawa, T. Sugimoto, S. Nomura, J. Electrochem. Soc. 150 (2003) A616.
[8] H. Nakajima, S. Nomura, T. Sugimoto, S. Nishikawa, I. Honma, J. Electrochem. Soc. 149 (2002) A953.
[9] M.T. Pope, A. Müller (Eds.), Polyoxometalate Chemistry: From Topology Via Self-Assembly to Applications, Kluwer Academic Publishers, Dordrecht, 2001.
[10] O. Nakamura, T. Kodama, I. Ogino, Y. Miyake, Chem. Lett. 1 (1979) 17.
[11] R.C.T. Slade, M.J. Omana, Solid State Ionics 58 (1992) 195.
[12] G.M. Brown, M.-R. Noe-Spirlet, W.R. Busing, H.A. Levy, Acta Cryst. B33 (1977) 1038.
[13] R.C.T. Slade, H.A. Pressman, E. Skou, Solid State Ionics 38 (1990) 207.
[14] U. Mioc, M. Davidovic, N. Tjapkin, P. Colomban, A. Novak, Solid State Ionics 46 (1991) 103.
[15] O. Nakamura, Prog. Batteries Solar Cells 4 (1982) 230.
[16] S. Malhotra, R. Datta, J. Electrochem. Soc. 144 (1997) L23.
[17] V. Ramani, H.R. Kunz, J.M. Fenton, J. Membr. Sci. 232 (2004) 31.
[18] B. Tazi, O. Savadogo, J. New Mater. Electrochem. Syst. 4 (2001) 187.
[19] Y.S. Kim, F. Wang, M. Hickner, T.A. Zawodzinski, J.E. McGrath, J. Membr. Sci. 212 (2003) 263.
[20] M.A. Sweikart, A.M. Herring, J.A. Turner, D.L. Williamson, B.D. McCloskey, S.R. Boonrueng, M. Sanchez, J. Electrochem. Soc. (2004) in press.
[21] P. Staiti, Mater. Lett. 47 (2001) 241.
[22] P. Staiti, J. New Mater. Mater. Electrochem. Syst. 4 (2001) 181.
[23] I. Honma, H. Nakajima, O. Nishikawa, T. Sugimoto, S. Nomura, Solid State Ionics 162–163 (2003) 237.
[24] I. Honma, H. Nakajima, O. Nishikawa, T. Sugimoto, S. Nomura, J. Electrochem. Soc. 149 (2002) A1389.
[25] I. Honma, H. Nakajima, S. Nomura, Solid State Ionics 154–155 (2002) 707.
[26] U. Lavrencic Stangar, N. Grošelj, B. Orel, A. Schmitz, P. Colomban, Solid State Ionics 145 (2001) 109.
[27] I. Honma, Y. Takeda, J.M. Bae, Solid State Ionics 120 (1999) 255.
[28] U. Lavrencic Stangar, N. Groselj, B. Orel, P. Colomban, Chem. Mater. 12 (2000) 3745.
[29] J.-D. Kim, I. Honma, Electrochim. Acta 49 (2004) 3429.
[30] C.R. Mayer, R. Thouvenot, Chem. Mater. 12 (2000) 257.
[31] C.R. Mayer, R. Thouvenot, T. Lalot, Macromolecules 33 (2000) 4433.
[32] R.C. Schroden, C.F. Blanford, B.J. Melde, B.J.S. Johnson, A. Stein, Chem. Mater. 13 (2001) 1074.
[33] P. Judeinstein, Chem. Mater. 4 (1992) 4.
[34] D.E. Katsoulis, Chem. Rev. 98 (1998) 359.
[35] I. Honma, S. Nomura, H. Nakajima, J. Membr. Sci. 185 (2001) 83.
[36] Y. Jeannin, J. Martin-Frere, in: A.P. Ginsberg (Ed.), Inorganic Syntheses, vol. 27, Wiley, 1990, p. 111.
[37] C.M. Tourne, G.F. Tourne, S.A. Malik, T.J.R. Weakley, J. Inorg. Nucl. Chem. 32 (1970) 3875.
[38] J.E. Tanner, J. Chem. Phys. 52 (1970) 2523.
[39] K.G. Helmer, M.D. Hurlimann, T.M. Deswiet, P.N. Sen, C.H. Sotak, J. Magn. Reson., Ser. A 115 (1995) 257.
[40] O. Kratky, Small Angle X-Ray Scattering, Academic Press, New York, 1982.
[41] D.L. Williamson, Mater. Res. Soc. Symp. Proc. 251 (1995) 377.
[42] V. Mehta, J.S. Cooper, J. Power Sources 114 (2003) 32.
[43] C. Rocchiccioli-Deltcheff, M. Fournier, R. Franck, R. Thouvenot, Inorg. Chem. 22 (1983) 207.
[44] C. Pazé, S. Bordiga, A. Zecchina, Langmuir 16 (2000) 8139.
[45] A. Mazeaud, Y. Dromzee, R. Thouvenot, Inorg. Chem. 39 (2000) 4735.